Prototype Parallel Readout System for Position Sensitive PMT based Gamma Ray Imaging Systems

Frezghi Habte, *Member IEEE*, Peter D. Olcott, Craig S. Levin, *Member IEEE*, Angela M. Foudray, *Student Member IEEE* and Jonathon A. Talcott, *Student Member IEEE*

***Abstract*-- A fully parallel prototype readout system that allows digitization and acquisition of 64 or more anode signals from a position sensitive photomultiplier tube (PSPMT) was developed for miniature hand-held gamma camera. This acquisition system was developed to study the benefits of a fully digital readout system compared to charge multiplexed techniques such as resistive division. The system is based on the CAMAC instrumentation standard and is controlled via a Macintosh Computer. Four 16-channel charge-to-digital conversion (QDC) CAMAC modules were used to digitize individual anode signals from the PSPMT. To maximize the data transfer rate, a list processor module is also added in the system. Kmax software from SPARROW is used for acquisition and processing of the digitized data. The system provided greater than 0.5% improvement in linearity and ~ 3% improvement in energy resolution when a gain correction is applied to list-mode data. More than 6% improvement in linearity, better image quality with 16:1 peak to valley ratio, and higher edge sensitivity is obtained compared to resistive division readout method.**

I. INTRODUCTION

Miniature hand-held gamma camera is being developed for surgical cancer staging [1]. It is based on 5x5cm^2 imaging field of view (FOV) position sensitive photomultiplier tube (PSPMT) and discrete LSO scintillation crystal detector system. Due to high signal-to-noise ratio, PSPMTs are the most commonly used photodetectors in many imaging applications ranging from compact imaging probes to small animal PET scanners [2- 5].

The readout of PSPMT based detector system is typically performed using charge division techniques [6,7] to provide a relatively simple electronics solution. On the other hand, the non-uniform spatial response and gain variation of PSPMT within a small field-of-view (FOV) significantly degrades performance unless individual anode correction is applied. As reported in [8] charge division based readout system has limitations in accurate localization of events and can cause resolution degradation. The edge effects inherent to this method also limit the useful FOV. The main advantage of independent channel readout is that it allows digital correction of gain variation, cross-talk and non-uniformity within the readout channels providing accurate position estimation and image quality. A drawback is that it requires more supporting electronics. But due to the advances and novel developments in the technology of digitizer chips and integrated circuits, this is no longer a great impediment.

This work focuses on the development of a prototype multi-channel readout system for studying advantages of a fully parallel readout system compared to charge multiplexing techniques.

II. MATERIALS AND METHODS

A. Readout System description

Our compact gamma camera is based on the Hamamatsu H8500 PSPMT detector equipped with 64 (8 x 8) anode pixels in a 50 mm square active detector area. This detector will be coupled to a configuration of collimator and LSO scintillation crystal array optimized for photon detection sensitivity and resolution [9]. The signal output from each anode is read out individually using a CAMAC based acquisition system as depicted in Figure 1. Four charge-to-digital converters (QDCs) (Phillips Scientific model 7166), each with 16-channels are used to digitize the signals from all 64 channels of the PSPMT detector. The signal from the last dynode is inverted and used to generate a fast gate signal to trigger an acquisition of an event in the QDCs. The delay between the analog input signals and gate signal was adjusted using a delay board built from discrete delay components. The input charge from each anode within the QDC is first integrated and digitized in parallel to register an event. The integration time is determined by the gate width, which can be adjusted to an optimal value. A minimum of 7.2μS conversation time is required for each channel of QDC, which is the fundamental limit to the sampling rate. The delayed analog signals are coupled directly to the QDC inputs without amplification or shaping. The digital data is transported in real time to a G4 power Mac via SCSI bus Controller (Jorway 73A). To maximize the data rate

Manuscript received October 30, 2003. This was supported by a research grant (RG –01-0492) from the Whitaker Foundation.

F.Habte is with the VA Medical Center and the University of California San Diego (UCSD) School of Medicine, Department of Radiology, San Diego CA 92161 USA (telephone: 858-552-8585 ext. 3594, e-mail: fhabte@ucsd.edu).

P.D.Olcott is with the UCSD Computer Science Department and the VA Medical Center, La Jolla, CA 92093 USA. (telephone:858-552-8585 x5364, e-mail: polcott@ucsd.edu).

C. S. Levin is with the VA Medical Center and the University of California San Diego (UCSD) School of Medicine, Department of Radiology, San Diego CA 92161 USA (telephone: 858-552-7511, e-mail: clevin@ucsd.edu).

A. M. Foudray, is with the UCSD Physics Department and the VA Medical Center, La Jolla, CA 92093 USA. (telephone: 858-552-8585 ext. 5364, e-mail:aklohs@physics.ucsd.edu).

J. A. Talcott is with the UCSD Electrical Engineering Department and the VA Medical Center, San Diego, CA 92161 USA. (telephone: 858-552-8585 ext. 5364, e-mail: jtalcott@ucsd.edu).

a List Processor (Hytec Electronics Ltd LP 1342) is also included in the CAMAC system.

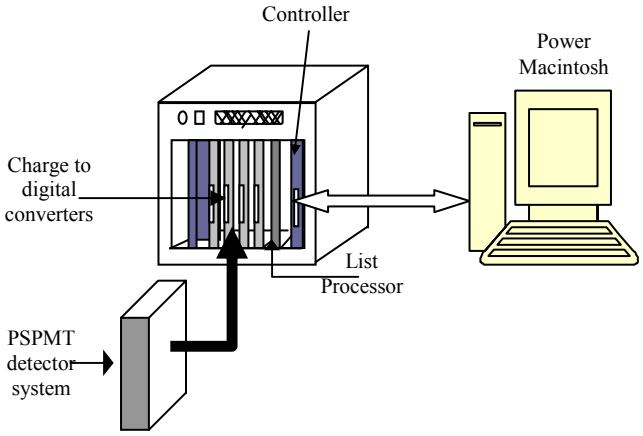

Figure 1: Experimental Setup of CAMAC based fully parallel readout and acquisition system

B. *Software Implementation*

The digitized data is acquired and processed in a Mac using Kmax software tools [10], which is based on a simplified built-in script language significantly simplifying the software implementation. Kmax allows non-buffered (event by event) or buffered acquisition options. In either case, the event is acquired and sorted in real-time and/or saved in list mode data for off-line processing**.** Data synchronization is performed by applying a global CAMAC clear command. This generates large dead time (on the order of a millisecond) significantly limiting the count rate performance. We are currently investigating remedies to this problem. The list mode data is processed off-line using Matlab. Event positioning was performed using a weighted mean algorithm.

III. MEASUREMENT AND RESULTS

A. *Gain variation profile*

The gain variation within the 64 anodes of the H8500 PSPMT was measured using a green LED light source at a distance of 40cm from the face of the PSPMT. The high voltage was set to –1000V. The list mode data from all anode signals were acquired and sorted according to anode pulse height. Normalized gain variation was determined from the peak location in the pulse height histogram for each anode (Figure 2). The maximum gain variation between anodes was roughly 45%.

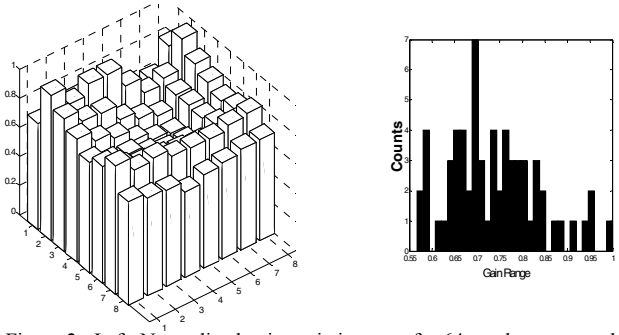

Figure 2: Left: Normalized gain variation map for 64 anodes measured from flood irradiation using LED light source. Right: The anode gain variation histogram.

B. *Flood image, linearity and crystal identification*

The system was tested using a 23x23 LSO array of 2x2x3 mm^3 crystals. Four layers of Teflon tape cover each crystal face except the side coupled to the PSPMT. The crystal array was coupled to the PSPMT using silicon based optical grease. The detector system was flood irradiated using a ^{57}Co source (122keV). Figure 3 shows the crystal map, cross-section profile and linearity plot before gain correction is applied. All crystals (i.e. 21x21 crystals) within the active FOV of the PSPMT are visible with dynamic range extending to the FOV edges. Due to lower light collection at the edge of the PSPMT FOV, the edge of the dynamic range is slightly compressed and the edge crystals are pushed inwards slightly. Otherwise good image quality with 13:1 average peak to valley ratio was obtained. Spatial linearity, measured from plotting the true vs. mapped crystal position was excellent (> 99%).

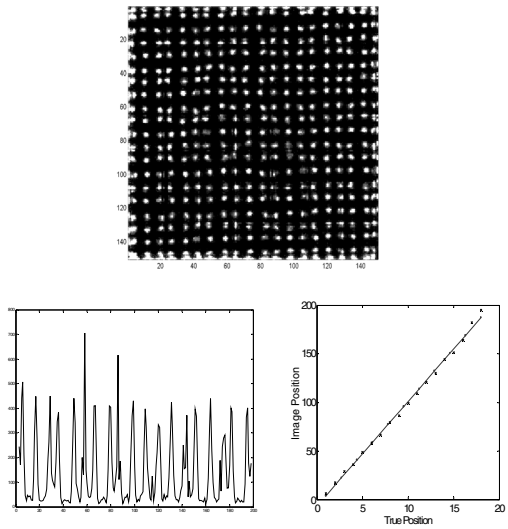

Figure 3: **Top**, Crystal array flood map using ^{57}Co source without gain correction. **Bottom Left**, Cross section profile across the central row. **Bottom Right,** Corresponding linearity curve true crystal location versus that seen in the image across the central row.

Figure 4 shows the flood image of the crystal map after gain correction. Both the image quality and the linearity were improved after the correction. An average peak to valley ratio of 16:1 was obtained with much less image distortion compared to that observed before gain correction. An even higher degree of spatial linearity (>99.9%) was observed. Crystal boundaries were drawn around the peak location of the flood image using a crystal segmentation algorithm from which the individual crystal counts and energy resolution are extracted. An analysis of the crystal count variations indicates good image uniformity for all visible crystals. This boundary may be used to generate lookup tables to correct spatial linearity and uniformity and to determine the event energy over the array.

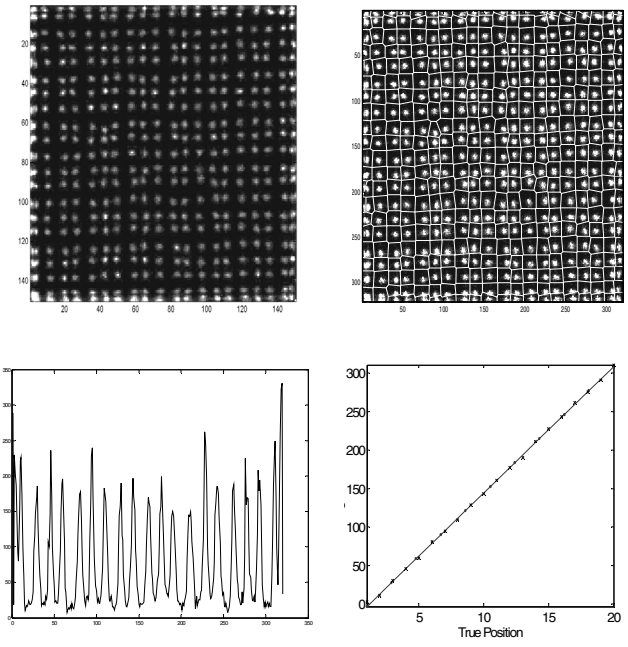

Figure 4**: Top Left,** Crystal map after gain correction**. Top Right,** Crystal map boundaries drawn from crystal peak positions in image**. Bottom Left,** Cross-section profile across the central row. **Bottom Right**, Linearity curve across the central row: true crystal position versus crystal location in flood image.

C. Energy Resolution

Energy resolution for each anode of the PSPMT was measured for a single LSO crystal directly coupled to the center of each anode. The single anode energy spectrum for a typical crystal is shown in figure 5. The energy resolution, measured by a Gaussian fit to the 122 keV photopeak, ranges from 21% to 29% with an average value of 25%. For comparison, individual energy spectra were also extracted from the flood image shown in figure 4 by position gating from the segmented flood map. The calculated individual array crystal energy resolutions range from 27% to 34% with average value of 30%, which is slightly worse than for the case of single crystal coupled to a single anode since for the array, light from any one crystal is shared between multiple anodes and the dead spaces between the anodes of the PSPMT.

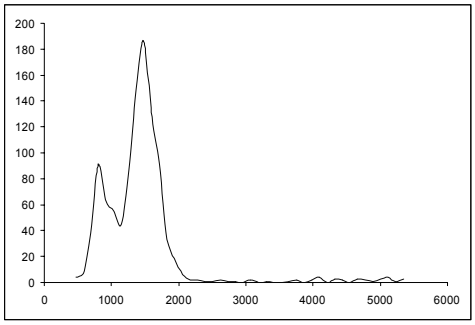

Figure 5: Sample ^{57}Co energy spectra for single 2x2x3 mm^3 LSO crystal coupled to a single anode.

D. Spatial resolution

Spatial resolution measurement was performed by stepping a collimated source of ^{57}Co with beam spot size ~0.7mm in steps of 0.4mm steps across the middle row of a 5x5 array of 2x2x3 mm3 LSO crystals individually wrapped in Teflon tape. A spatial resolution of less than 2.6 mm FWHM was obtained as shown in figure 6. This value is a convolution of the rectangular crystal (2.0 mm) and beam spot (~0.7 mm) functions, which means that the spatial resolution is limited by the crystal size.

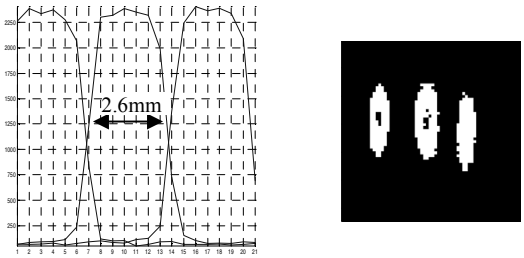

Figure 6: Left: Spatial resolution profiles through three crystals. Right: Resulting sum image from traversing three crystals.

E. Inter anode cross talk and light distribution

The crosstalk was measured in two ways. A 2x2x3 mm^3 LSO crystal was placed in several positions on the PSPMT. For each crystal location, the list-mode data of all anodes was recorded simultaneously. From this we generated both an inter-anode event distribution (2000 events) and the distribution of signals recorded in all anodes for just a single event. Figure 7 shows a sample of these inter-anode cross talk measurements (count distribution and light spread) for the case when the 2x2x3 mm^3 crystal was placed at the interface between four of the 5.6x5.6 mm^2 anodes. When the crystal was placed at the center of one anode more than 95% of the events are recorded only at that anode location. In all cases light output from each LSO crystal is highly localized and at most 9 anodes are involved in the light collection and

positioning for any event. We are currently implementing this local centroiding in our processing software.

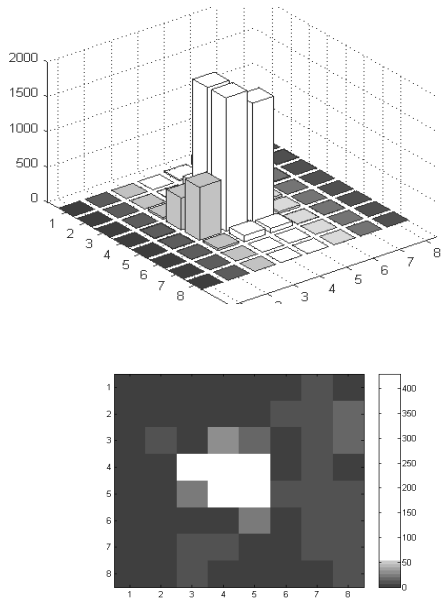

Figure 7: Cross-talk measurements. **Top**, histogram of events recorded, Bottom, light spread for single event. In this case the crystal was placed at the interface between four anodes.

IV. SUMMARY AND CONCLUSION

A fully parallel readout system that allows simultaneous digitization and acquisition of detector signals from a multi-anode PSPMT based detector system is being developed. Although we have focused our development on reading out a PSPMT, the system may be used for variety of imaging applications. The capability of digital control per channel allowed accurate gain correction that significantly improved system performance. Better than 6% improvement in spatial linearity was obtained compared to an improved resistive charge division system that is also under investigation [11]. A fully digital system provides better performance since it does not introduce distortion as in the case of resistive division due to resistive elements. In addition, full digitization allows channel-by-channel characterization and calibration of a detector system to optimize system performance. The system count rate performance could be improved also by applying a sparse readout method where only anodes above minimum threshold within the localized LSO light cone are used in the position estimation. A 2.6mm fwhm spatial resolution was obtained, which was determined by the crystal size and a 0.7mm photon beam spot size. Excellent flood image quality with 16:1 peak to valley ratio was also obtained.

V. REFERENCE

[1] C. S. Levin, P. D. Olcott, F. Habte, J. Talcott, A. Foudray and A. Dhanasopon. Miniature Gamma Ray Camera to Assist Surgical Staging of Cancer, Presented at the IEEE Nuclear Science Symposium and Medical Imaging Conference. Portland, 2003.

[2] R. Pani, et al., A novel compact gamma camera based on flat panel PMT, Nucl. Instr. And Meth. A 513 (2003) 36-41.

[3] C. S. Levin, Detector design issues for compact nuclear emission cameras dedicated to breast imaging, Nucl. Instr. And Meth. A 497 (2003) 60-74.

[4] J. Vaquero et. al., Performance Characteristics of a Compact Position-Sensitive LSO Detector, IEEE Trans. Med. Imag,, vol. 17, No. 6, December 1998.

[5] G.K. Loudos, et. al., Improving spatial resolution in SPECT with the combination of PSPMT based detector and iterative reconstruction algorithms, Computerized Medical Imaging and Graphics 27 (2003) 307-313.

[6] S. Siegel, R. W. Silverman, Y. Shao, and S. R. Cherry, Simple Charge Division Readouts for Imaging Scintillator Arrays using a Multi-Channel PMT, IEEE Trans. Nucl. Science, vl 43, No. 3, June 1996.

[7] J.L. Alberi and V. Radeka, Position sensing by charge division, IEEE Trans. Nucl. Science, vol 23, No. 1, Febraury 1976.

[8] R. Pani, et. al., Flat Panel PMT for photon emission imaging, Nucl. Instr and Meth. A 505 (2003) 590-594.

[9] A. P. Dhanasopon, C. S. Levin, A. M. Foudray, P. D. Olcott, J. A. Talcott and F. Habte, Scintillation Crystal Design Features for a Minature Gamma Ray Camera, Presented at the IEEE Nuclear Science Symposium and Medical Imaging Conference. Portland,

[10] Sparrow Corporation, Daytona Beach, FL, USA

[11] P. D. Olcott, J. A. Talcott, C. S. Levin, F. Habte and A. M. K. Foudray, Compact Readout Electronics for Position Sensitive Photomultiplier Tubes. Presented at the IEEE Nuclear Science Symposium and Medical Imaging Conference. Portland.